BIODIVERSITAS
Volume 27, Number 2, February 2026
Pages: 11

ISSN: 1412-033X
E-ISSN: 2085-4722
https://doi.org/10.13057/biodiv/d270228

Antibacterial activity and metabolite profiling of mangrove endophytic fungus *Talaromyces adpressus* from *Rhizophora apiculata*

ANAK AGUNG GEDE INDRANINGRAT[1,♥], PANDE PUTU CHRISTINE PUTRI PURNAMI[1], NI MADE AYU SUARDANI SINGAPURWA[2], MADE DHARMESTI WIJAYA[3]

[1]Department of Microbiology and Parasitology, Faculty of Medicine and Health Sciences, Universitas Warmadewa. Jl. Terompong No. 24, Denpasar 80235, Bali, Indonesia. Tel./fax.: +62361- 240-727, ♥email: indraningrat@warmadewa.ac.id

[2]Department of Food Science and Technology, Faculty of Agriculture, Science and Technology, Universitas Warmadewa. Jl. Terompong No. 24, Denpasar 80235, Bali, Indonesia

[3]Department of Pharmacology, Faculty of Medicine and Health Sciences, Universitas Warmadewa. Jl. Terompong No. 24, Denpasar 80235, Bali, Indonesia

Manuscript received: 30 October 2025. Revision accepted: 23 February 2026.

Abstract. *Indraningrat AAG, Purnami PPCP, Singapurwa NMAS, Wijaya MD. 2026. Antibacterial activity and metabolite profiling of mangrove endophytic fungus* Talaromyces adpressus *from* Rhizophora apiculata*. Biodiversitas 27 (2): d270228. https://doi.org/10.13057/biodiv/d270228.* Antimicrobial resistance (AMR) continues to pose a major global health threat and has driven the exploration of under-studied ecosystems, including mangrove forests, as sources of bioactive microorganisms. Therefore, this study aimed to isolate and identify endophytic fungi associated with mangrove roots and to evaluate the antibacterial activity and GC-MS-based metabolite profile of a selected isolate against multidrug-resistant (MDR) bacterial pathogens. The isolate was identified based on morphological characteristics and confirmed by ITS rDNA sequencing, showing 100% similarity to *Talaromyces adpressus*. Crude ethyl acetate extract obtained from submerged fermentation culture was screened for antibacterial activity against multidrug-resistant (MDR) bacteria, including methicillin-resistant *Staphylococcus aureus* (MRSA) and extended-spectrum β-lactamase (ESBL)-producing *Escherichia coli*, *Klebsiella pneumoniae*, and *Acinetobacter baumannii*. Agar disc diffusion assays showed measurable inhibition zones of 13.22±1.13 mm (MRSA), 10.41±1.54 mm (ESBL-*E. coli*), 10.05±1.85 mm (ESBL-*A. baumannii*), and 9.98±0.11 mm (ESBL-*K. pneumoniae*). However, broth microdilution assays revealed minimum inhibitory and bactericidal concentrations exceeding 512 µg mL^{-1} for all tested strains, indicating weak antibacterial potency of the crude extract in liquid culture. GC-MS profiling tentatively identified ten major metabolites, including fatty acids (lauric, myristic, palmitic, oleic acids), diketopiperazines [cyclo(L-Pro-L-Val), cyclo(Phe-Pro)], phenethyl alcohol, phenylacetic acid, 2,4-di-tert-butylphenol, and ergosterol, which have been reported to possess antimicrobial or signaling-modulatory properties. Overall, these findings expand the ecological record of *T. adpressus* in mangrove ecosystems and provide preliminary antibacterial screening and chemical profiling data, highlighting the need for further fractionation and compound-level validation in future studies. To the best of our knowledge, this is the first report of isolation and characterization of endophytic fungus *T. adpressus* A1RA from roots of *R. apiculata* Blume collected from the Ngurah Rai Mangrove Forest, Bali, Indonesia.

Keywords: Antibacterial activity, fungal endophyte, mangrove ecosystems, *Rhizophora apiculata*, *Talaromyces adpressus*

INTRODUCTION

Antimicrobial resistance (AMR) has emerged as one of the greatest global health challenges, causing 1.27 million deaths annually and associated with nearly 5 million deaths worldwide in 2019 (Alhassan and Abdallah 2024). The World Health Organization (WHO) has identified AMR as one of the top ten threats to global health, with resistant pathogens undermining the effectiveness of existing antibiotics and driving increases in morbidity, mortality, and economic burden (Dadgostar 2019). Without new therapeutic options, the global economic loss from AMR could reach US$100 trillion by 2050 (Gulumbe et al. 2022). These figures underscore the urgent need to explore alternative sources of antimicrobial compounds, especially natural products (Newman and Cragg 2020).

Among the most concerning pathogens are methicillin-resistant *Staphylococcus aureus* (MRSA), ESBL-producing *Escherichia coli* and *Klebsiella pneumoniae* (Tacconelli et al. 2018). These bacteria are included on WHO's priority list due to their multidrug resistance and high prevalence in hospitals and communities (Santajit and Indrawattana 2016). In Indonesia and Southeast Asia, the prevalence of ESBL-producing Enterobacteriaceae is often above 40% in clinical isolates, while MRSA remains a common cause of life-threatening infections (Liana et al. 2022; Kadariswantiningsih et al. 2025). These circumstances necessitate the discovery of new antimicrobial agents from underexplored ecosystems (Genilloud 2019).

Microorganisms remain the dominant source of antibiotics, with more than 65% of approved drugs derived from microbial natural products (Newman and Cragg 2020). Fungi are prolific producers of structurally diverse metabolites with antibacterial, antifungal, anticancer, and immunomodulatory activities (Keller 2019). Endophytic fungi, which inhabit plant tissues without causing disease, are recognized as particularly valuable due to their ability to synthesize novel metabolites shaped by their host and environment (Nagarajan et al. 2021; Galindo-Solís and Fernández 2022). Their ecological adaptation often leads to

chemical diversity not observed in terrestrial fungi (Liao et al. 2025).

Mangrove forests are harsh intertidal ecosystems with fluctuating salinity, anoxic soils, and tidal stress, conditions that drive unique metabolic adaptations in associated organisms (Chen et al. 2019; Madhavan et al. 2025). Mangrove endophytic fungi produce bioactive compounds such as azaphilones, isocoumarins, polyketides, and lycorine with antimicrobial and cytotoxic potential (Zhang et al. 2022; Nasution et al. 2024; Ortega et al. 2025). Although Southeast Asian mangroves are biodiversity hotspots, their fungal diversity remains poorly explored (Buenavista and Purnobasuki 2023). This diversity is valuable both ecologically and pharmacologically (Guerrero et al. 2025), and these fungi may provide promising candidates for antimicrobial screening, although compound-level validation is still required.

The genus *Talaromyces* is globally distributed and known to produce diverse secondary metabolites, including polyketides, azaphilones, and diketopiperazines (Zhai et al. 2016; Nicoletti et al. 2023). Several species have shown promising bioactivities: *T. stipitatus* produces terrein with antibacterial and cytotoxic effects (Cai et al. 2017), *T. purpurogenus* produces antimicrobial azaphilones (Chen et al. 2020), and *T. pinophilus* produces diketopiperazines that inhibit quorum sensing (Nicoletti et al. 2023). *Talaromyces adpressus* also produces bioactive compounds, including sterigmatocystin, with reported antitumor, antibacterial, antifungal, and anti-inflammatory activities (Zheng et al. 2023; Shi et al. 2024; Bao et al. 2025). However, its occurrence in mangrove endophytes and the chemical profile and antibacterial potential of mangrove-derived isolates remain unreported.

To date, information on the chemical profile of *T. adpressus* from mangrove environments remains limited. The stressful mangrove environment may induce metabolite production not found in terrestrial isolates (Hastuti et al. 2020; Nizam et al. 2022). Moreover, no chemical profiling studies, such as GC/MS, have examined this species. Given the global urgency of AMR, investigating underexplored fungal taxa such as *T. adpressus* is timely and relevant (Oliveira et al. 2024). In this context, chemical profiling serves as an initial exploratory step rather than definitive identification of bioactive principles.

To address the AMR challenge, the aim of this study was to (i) isolate and identify isolates of *T. adpressus* using a polyphasic approach combining morphology, ITS sequencing, and phylogenetic analysis; (ii) screen its ethyl acetate extract against multidrug-resistant bacteria including MRSA and ESBL-producing *E. coli, K. pneumoniae*, and *A. baumannii*; and (iii) profile its major metabolites using GC-MS as an initial chemical overview.

MATERIALS AND METHODS

Study area

Mangrove samples were collected in June 2024 from the Ngurah Rai Mangrove Forest located in southern Bali, Indonesia (8°41′22.1″S, 115°12′34.8″E). This conservation area spans approximately 1,373 ha and is one of the largest protected mangrove ecosystems in Bali. The site experiences tropical monsoon climate conditions, with average annual temperatures of 27-30°C and rainfall exceeding 2,000 mm. Salinity levels in the soil and surrounding waters fluctuate between 10-30 ppt depending on tidal cycles. The dominant mangrove flora includes *Sonneratia alba*, *Rhizophora apiculata*, *Avicennia marina*, and *Bruguiera gymnorhiza*. For this study, healthy, mature, and undamaged roots of *R. apiculata* were targeted as the source of endophytic fungi. The exact age of the sampled *R. apiculata* trees could not be determined because stand-level age records were unavailable for the sampling site. To minimize variability, sampling was restricted to visibly mature trees with well-developed root systems and intact canopies, and all samples were collected from the same stand area during a single sampling period. Samples were collected aseptically using sterilized scissors and placed in sterile polyethylene bags. To prevent contamination, the bags were transported in ice boxes to the Research Laboratory, Faculty of Medicine and Health Sciences, Universitas Warmadewa. All subsequent procedures were conducted under aseptic conditions in a laminar flow hood.

Isolation of endophytic fungi

Root samples were gently rinsed under running tap water to remove adhering soil particles and cut into segments of approximately 0.5-1.0 cm. Root tissues were taken from small-diameter root portions (fine-root scale) rather than thick prop roots to facilitate surface sterilization and endophyte emergence. Surface sterilization was performed by sequential immersion in 70% ethanol (1 min) and 1% sodium hypochlorite (3 min), followed by three rinses with sterile distilled water. Sterilized 2 mm root segments were placed on potato dextrose agar (PDA; five segments per plate) and incubated at 28°C for 7-14 days in the dark. Emerging hyphae were sub-cultured to PDA to obtain pure isolates.

Identification of fungi by light microscope and scanning electron microscope

The morphological structures of isolate A1RA were examined using both compound light microscopy and scanning electron microscopy (SEM). For light microscopy, a compound microscope equipped with a Leica ICC50 E digital camera system was used. Fungal mounts were prepared by transferring a small portion of actively growing mycelium to a glass slide, staining with lactophenol cotton blue, and gently placing a coverslip to avoid air bubbles. Observations were performed under bright-field illumination at magnifications ranging from 100× to 400×. Digital micrographs were acquired using the Leica ICC50 E camera (5.0-megapixel sensor; live imaging up to 30 fps; Leica LAS EZ software compatibility), enabling visualization of hyphae, conidiophores, and conidia.

The morphology of fungal isolate A1RA was examined using scanning electron microscopy at the MERO Foundation (https://www.merofoundation.org/). The fungal colonies grown on agar medium was first fixed in 2% glutaraldehyde followed by post fixation in 1% osmium

tetroxide. Samples were then dehydrated through a graded ethanol series to remove residual water and air-dried at room temperature. Dried samples were sputter-coated with a thin layer of gold to enhance surface conductivity, mounted onto aluminium stubs using carbon tape, and examined under a JEOL JSM-IT200 scanning electron microscope operated in high vacuum mode. Imaging was conducted at an accelerating voltage of 10.0 kV, a probe current of 30.0 pA, and a working distance of 9.0-11.8 mm. Micrographs were taken at magnifications of 3,000×, 10,000×, and 20,000× with scale bars of 5 or 1 µm. The images were used to observe hyphal and spore structures to support morphological identification of fungal colonies A1RA.

Preliminary antibacterial screening

This screening was performed using the agar-block (agar plug) assay. 5 mm PDA blocks bearing actively growing mycelia from the colony margin of a 7-day-old PDA culture of isolate A1RA were placed onto Luria Bertani agar lawns of the test bacteria and incubated at 35 ± 2°C for 18-24 h; inhibition zones (mm) were recorded. Only isolates showing reproducible inhibition against ≥1 test bacterium, which were designated as "potential" and advanced. Based on this screen, isolate A1RA was selected for molecular identification and subsequent chemical and antibacterial analysis.

Molecular identification and phylogenetic analysis

Genomic DNA was extracted from isolate A1RA using the Quick-DNA Magbead Plus Kit (Zymo Research, D4082). The internal transcribed spacer (ITS) region of rDNA was amplified using primers ITS1 (5′-TCCGTAGGTGAACCTGCGG-3′) and ITS4 (5′-TCCTCCGCTTATTGATATGC-3′) in a 25 µL PCR mixture containing 1× PCR buffer, 2.5 mM $MgCl_2$, 0.2 mM dNTPs, 0.4 µM of each primer, 1 U Taq DNA polymerase, and approximately 50 ng of template DNA. The thermocycling program consisted of an initial denaturation at 95°C for 5 min; 35 cycles of 95°C for 30 s, 55°C for 30 s, and 72°C for 1 min; followed by a final extension at 72°C for 10 min. PCR products were visualized on a 1.2% agarose gel, purified, and sequenced bidirectionally by PT Genetika Science (Jakarta, Indonesia). The resulting ITS sequence was analysed using BLASTn against the NCBI GenBank database. The sequence was deposited in GenBank under accession number (PX480240), confirming the molecular identity of isolate A1RA. The obtained sequence was compared with GenBank database entries using BLASTn. Phylogenetic analysis was performed using MEGA X software with the neighbor-joining method and 1,000 bootstrap replications. To construct a robust reference dataset, nine ITS sequences derived from authenticated type material were downloaded from the NCBI database, including seven species belonging to the genus *Talaromyces*. Two ITS sequences from *Penicillium chrysogenum* and *Penicillium rubens* were included as outgroup taxa to root and stabilize the phylogenetic tree. Multiple sequence alignment was conducted using MUSCLE in MEGA X before generating the phylogenetic tree.

Fermentation and extraction of metabolites

The identified fungus A1RA was cultured in Sabouraud Dextrose Broth (SDB). For seed culture preparation, small mycelial plugs from actively growing PDA plates were inoculated into 10 mL SDB and incubated at 28°C, 150 rpm for 7 days with gentle agitation. For larger-scale fermentation, 90 mL of sterile SDB was dispensed into 250 mL Erlenmeyer flask, each inoculated with 10 mL of seed culture. Flasks were incubated in a shaker at 28°C, 150 rpm for 14 days to allow for optimal secondary metabolite production. At the end of incubation, cultures were filtered through Whatman filter paper no 1 (Cytiva, China) to separate mycelia from broth. After filtration, only the culture filtrate was extracted three times with an equal volume of ethyl acetate (EtOAc) in a separatory funnel, while mycelial biomass was discarded. The pooled organic phases were concentrated and evaporated under reduced pressure at 40°C using a rotary evaporator (Heidolph, Germany), yielding 112 mg of crude extract from 100 mL of culture filtrate and the extract was stored at 4°C until further use. Ethyl acetate was selected as the extraction solvent because it efficiently recovers semi-polar secondary metabolites commonly associated with fungal antibacterial activity while minimizing excessive co-extraction of polar media components.

Antibacterial assay

The antibacterial activity of A1RA extract was evaluated using an agar disc diffusion assay. Sterile paper discs (6 mm diameter, Oxoid, UK) were impregnated with 20 µL of extract solution prepared at a concentration of 50 mg/mL (equivalent to 1 mg extract per disc) and air-dried. Discs were then placed onto Luria Bertani agar plates seeded with test organisms at 0.5 McFarland turbidity (~1.5×10^8 CFU/mL). Test organisms included methicillin-resistant *S. aureus* (MRSA), ESBL-producing *E. coli*, ESBL-producing *K. pneumoniae*, and ESBL *A. baumannii* obtained from the culture collection of the Research Laboratory, Universitas Warmadewa. Levofloxacin (5 µg/disc) served as the positive control, while ethyl acetate was used as the negative control. Plates were incubated at 37°C for 24 h. Zones of inhibition were measured in millimetres using a digital calliper. All tests were conducted in triplicate, and results were expressed as mean ± standard deviation (SD).

MIC/MBC analysis

The minimum inhibitory concentration (MIC) and minimum bactericidal concentration (MBC) of the A1RA crude extract were determined using the standard broth microdilution method in 96-well microplates. Four multidrug-resistant bacterial isolates were tested (*S. aureus* MRSA, *E. coli* ESBL, *K. pneumoniae* ESBL, and *A. baumannii* ESBL). Each isolate was cultured on Mueller-Hinton Agar (MHA) for 24 h at 37°C, and colonies were suspended in 0.85% NaCl, adjusted to a 0.5 McFarland standard, and diluted in Mueller-Hinton Broth (MHB; Oxoid) to obtain a final inoculum of approximately 5×10^5 CFU/mL per well. The extract was dissolved in DMSO and serially diluted in MHB to yield final test concentrations of 32-512 µg/mL, with the final DMSO concentration maintained at ≤1% as

the solvent control. Positive control wells contained levofloxacin prepared at the same dilution range, while growth and sterility controls consisted of inoculated and uninoculated MHB, respectively. After adding the bacterial inoculum to the extract dilutions, the plates were incubated at 37°C for 20 h. The MIC was determined as the lowest concentration showing no visible turbidity relative to the growth control, while optical density at 600 nm (OD600) was used only to support visual observations. For MBC determination, 10 µL from wells without visible growth (MIC and higher concentrations) was streaked onto fresh MHA and incubated for 24 h. The MBC was defined as the lowest concentration that produced no colony growth. MIC and MBC determinations were performed in duplicate.

Gas chromatography-Mass spectrometry (GC/MS) analysis

The chemical composition of crude EtOAc extract was analysed using GC/MS at the Forensic Laboratory, Bali Regional Police. An Agilent 7890B GC system coupled with a 5977B Mass Selective Detector was employed. Separation was performed using an HP-5ms Ultra Inert column (30 m × 250 µm × 0.25 µm). Helium was used as the carrier gas at a constant flow of 2.9 mL/min. The oven temperature was programmed as follows: initial temperature 70°C (held for 5 min), ramped to 290°C at 10°C/min, and held for 3 min. The injector temperature was set at 290°C with splitless injection mode, and injection volume was 1 µL. The mass spectrometer was operated in electron ionization mode at 70 eV, with an ion source temperature of 230°C, quadrupole temperature of 150°C, and scanning range of m/z 50-550. Chromatograms and mass spectra were analysed using Agilent ChemStation software. Peaks were identified by comparison with NIST and Wiley spectral libraries. All compound identifications should therefore be regarded as tentative and based on spectral library matching rather than definitive structural confirmation. Tentative identification was further supported by literature data on retention times and mass fragmentation patterns. Out of the 64 peaks detected in the total ion chromatogram, the ten compounds with the highest relative peak areas were selected to provide an overview of the major detectable constituents of the crude extract, including both dominant and functionally relevant metabolites reported to possess antibacterial or signalling-related activities. Relative peak areas were calculated by dividing each peak's area by the sum of all peak areas, because the area of a peak was proportional to the amount of the compound in the sample. Only compounds with similarity indices above 85% were considered reliable identifications. All data generated or analysed during this study are included in this published article.

Data analysis

All experiments were conducted in replicate to ensure reproducibility; disc diffusion assays were performed in triplicate, whereas MIC/MBC determinations were conducted in duplicate. Data for antibacterial activity were expressed as mean ± SD. Statistical analysis was performed using SPSS version 26.0 (IBM, USA). One-way analysis of variance (ANOVA) was used to determine overall significance among groups, followed by Tukey's post hoc test for pairwise comparisons. A $p<0.05$ was considered statistically significant. Statistical analysis was applied only to disc diffusion inhibition zone data, whereas MIC and MBC values were interpreted descriptively because they represent categorical outcomes.

RESULTS AND DISCUSSION

Identification of fungi by light microscope and SEM

A total of four endophytic fungal isolates were recovered from surface-sterilized root tissues of *R. apiculata*. Preliminary antibacterial screening was conducted using the agar-block (agar plug) assay, and only isolate A1RA showed reproducible inhibition against ≥1 test bacterium was considered for further investigation. Cultivation of isolate A1RA on Potato Dextrose Agar (PDA) at 28°C for seven days resulted in extensive radial growth, with the colony spreading to the plate margins. The colony surface (upper surface) was white with a velvety to powdery texture and displayed concentric zonation with a slightly denser centre (Figure 1.A). The reverse side showed a distinct orange to reddish-orange pigmentation with concentric rings (Figure 1.B). These macroscopic features are consistent with the genus *Talaromyces*. These macroscopic features were further supported by microscopic and ultrastructural observations. Light microscopy using lactophenol cotton blue staining revealed septate hyphae and biverticillate conidiophores bearing metulae and phialides, which produced ellipsoidal conidia arranged in chains (Figure 2.A). Scanning electron microscopy confirmed these features, showing ellipsoidal conidia with finely roughened surfaces assembled in dense chains, characteristic of *T. adpressus* (Figures 2.B-2.C).

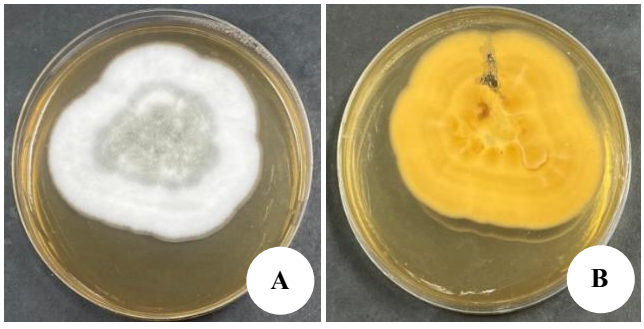

Figure 1. Morphological features of *Talaromyces adpressus* A1RA cultured on Potato Dextrose Agar (7 days, 28°C). A. Upper colony surface view showing a white, velvety to powdery colony with concentric zonation. B. Reverse surface view of the colony exhibiting orange to reddish-orange pigmentation with concentric rings

Molecular identification and phylogenetic analysis

The internal transcribed spacer (ITS) rDNA sequence of isolate A1RA showed 100% identity to *T. adpressus* via BLASTn analysis. Consistent with this result, the neighbor-joining phylogenetic tree placed A1RA within the *T. adpressus* clade, clustering closely with type and reference strains. *Penicillium chrysogenum* was used as the outgroup, and bootstrap values from 1,000 replications are shown at the nodes (Figure 3). The strong clustering pattern and supporting bootstrap values confirm the species-level assignment of isolate A1RA as *T. adpressus*. The close phylogenetic relationship of isolate A1RA with *T. adpressus* supported its identification at the species level.

Antibacterial screening

Following molecular confirmation, ethyl acetate extract of *T. adpressus* A1RA was evaluated for its antibacterial activity against multidrug-resistant bacterial strains. The ethyl acetate extract of *T. adpressus* A1RA produced measurable inhibition zones against all tested bacteria (Table 1). The largest inhibition zone was observed against methicillin-resistant *S. aureus* (MRSA) (13.22±1.13 mm), followed by *Streptococcus mutans* FNCC 0405 (12.43±0.79 mm) and *S. aureus* ATCC 25923 (12.08±0.28 mm). Inhibition was also recorded against ESBL-producing *Escherichia coli* (10.41±1.54 mm), ESBL-producing *A. baumannii* (10.05±1.85 mm), and *E. coli* ATCC 25922 (10.88±0.58 mm). Smaller inhibition zones were observed for *K. pneumoniae* ATCC 700603 (8.15±1.37 mm) and ESBL-producing *K. pneumoniae* (7.75±0.05 mm).

Agar plate observations (Figure 4) were consistent with the quantitative findings and confirmed the inhibitory activity of the extract against multidrug-resistant (MDR) bacteria. Clear inhibition zones were observed for MRSA and ESBL-producing *A. baumannii*, while ESBL-producing *E. coli* and ESBL-producing *K. pneumoniae* displayed narrower but visible halos. No inhibition was detected around the solvent control discs, whereas levofloxacin discs produced broad and distinctly clear zones.

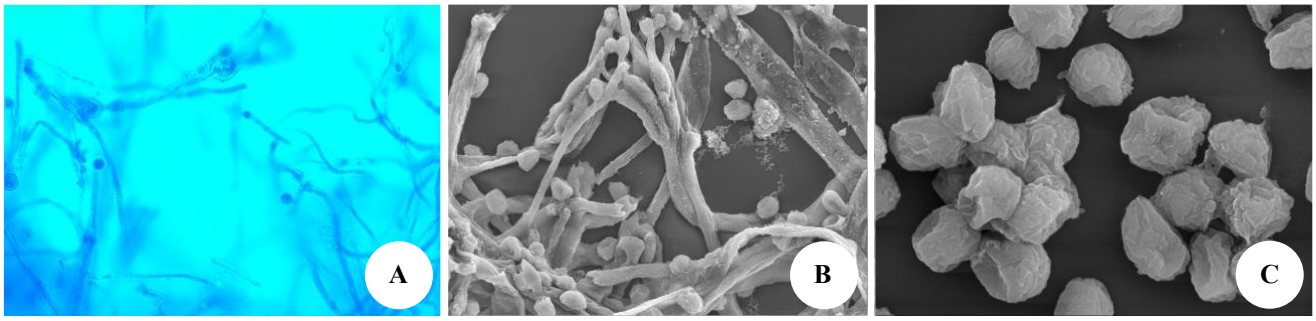

Figure 2. Microscopic and ultrastructural characteristics of *Talaromyces adpressus* A1RA. A. Light micrograph of septate hyphae and biverticillate conidiophores bearing chains of ellipsoidal conidia (100× magnification). B. Scanning electron micrograph showing hyphal structures with attached conidia (3,000× magnification). C. Scanning electron micrograph displaying individual ellipsoidal conidia with finely roughened surfaces (10,000× magnification)

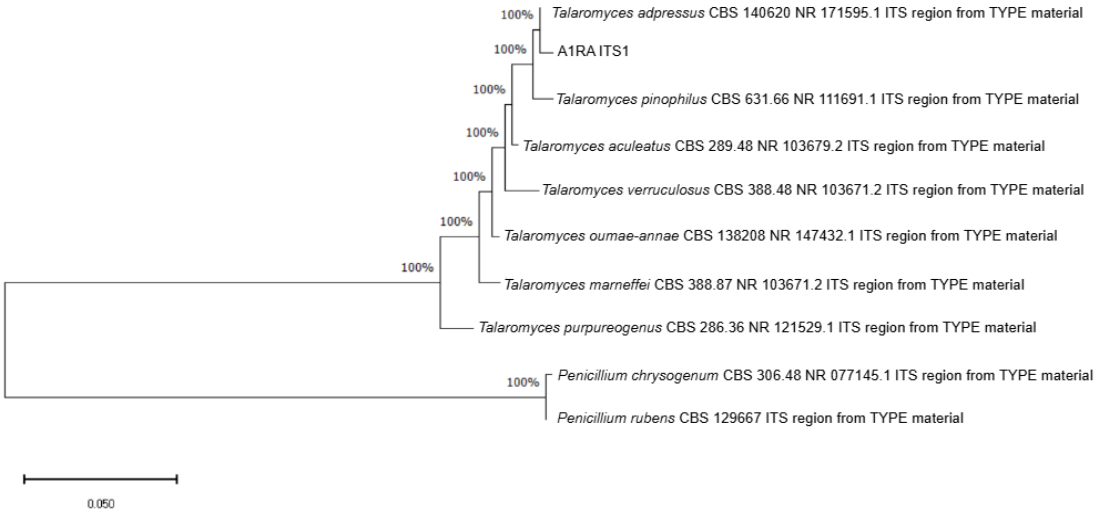

Figure 3. Neighbor-joining phylogenetic tree based on ITS rDNA sequences showing the placement of isolate A1RA within the *T. adpressus* clade. The analysis included ITS sequences from seven authenticated *Talaromyces* species and two *Penicillium* species (*P. chrysogenum* and *P. rubens*) used as outgroups. Bootstrap support values from the 1,000 replications are shown at the nodes. The scale bar represents 0.05 nucleotide substitutions per site

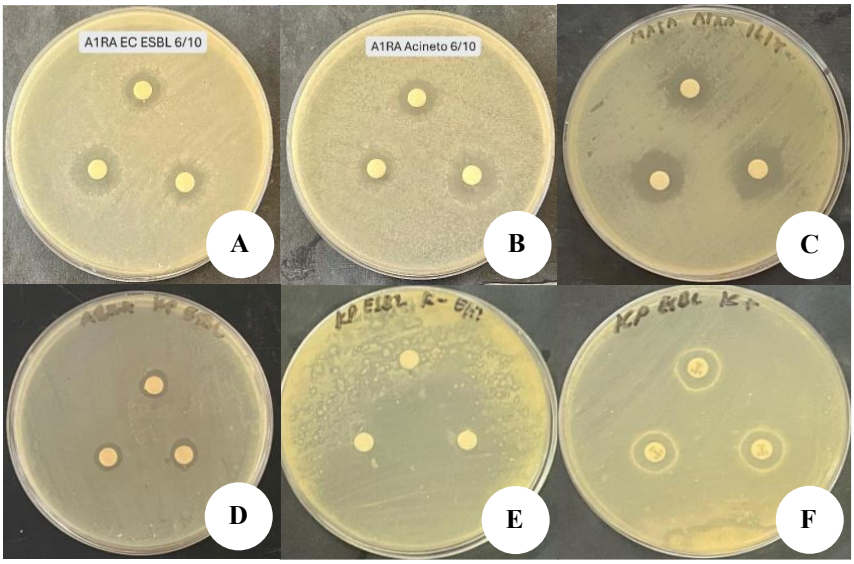

Figure 4. Disc-diffusion assay demonstrating the antibacterial activity of *T. adpressus* A1RA ethyl acetate extract against multidrug-resistant (MDR) clinical isolates. Inhibition zones were observed around extract-treated discs in: A. ESBL-producing *E. coli*, B. ESBL-producing *A. baumannii*, C. methicillin-resistant *S. aureus* (MRSA), D. ESBL-producing *K. pneumoniae*, E. Negative control (ethyl acetate), and F. Positive control levofloxacin tested against EBL producing *K. pneumoniae*

Table 1. Inhibition zone diameters (mm) of *T. adpressus A1RA* extract and controls against bacterial targets. Values represent mean ± SD of three replicates. Superscript letters indicate statistical differences among treatments; values with different letters within the same row are significantly different at $p < 0.05$ (one-way ANOVA followed by Tukey's HSD)

Bacterial isolates	EtOAc A1RA (Extract)	Levofloxacin (Positive control)	EtOAC (Negative control)
Staphylococcus aureus ATCC 25923	12.08±0.28^{b}	27.46±0.02^{a}	0.00±0.00^{c}
Streptococcus mutans FNCC 0405	12.43±0.79^{b}	27.22±0.64^{a}	0.00±0.00^{c}
Escherichia coli ATCC 25922	10.88±0.58^{b}	26.91±0.37^{a}	0.00±0.00^{c}
Klebsiella pneumoniae ATCC 700603	8.15±1.37^{b}	27.65±0.53^{a}	0.00±0.00^{c}
Methicillin-resistant *Staphylococcus aureus*	13.22±1.13^{a}	12.27±1.67^{a}	0.00±0.00^{b}
Escherichia coli ESBL	10.41±1.54^{b}	25.17±0.31^{a}	0.00±0.00^{c}
Klebsiella pneumoniae ESBL	9.88±0.11^{b}	13.70±0.20^{a}	0.00±0.00^{c}
Acinetobacter baumannii ESBL	10.05±1.85^{b}	18.06±0.22^{a}	0.00±0.00^{c}

MIC/MBC analysis

To further assess antibacterial potency, MIC and MBC assays were performed using broth microdilution method. The extract inhibited bacterial growth only at the highest concentration tested (512 µg/mL), while all lower concentrations allowed visible growth. Subculturing from wells without visible turbidity showed persistent colony formation at all concentrations, resulting in MBC values greater than 512 µg/mL for every isolate tested. Accordingly, the MIC and MBC for MRSA, ESBL-producing *E. coli*, *K. pneumoniae*, and *A. baumannii* were all recorded as >512 µg/mL, indicating the absence of sustained bacteriostatic or bactericidal effects within the tested concentration range (Table 2). These findings suggest that while the extract demonstrates measurable inhibitory zones in disc diffusion assays, its potency in broth microdilution is weak, with activity limited to high concentrations.

GC/MS) analysis

GC-MS profiling of A1RA ethyl acetate extract (Figure 5) revealed a chemically diverse metabolite spectrum with 64 peaks, of which 10 major compounds were tentatively identified. These metabolites included aromatic alcohols, phenolic derivatives, fatty acids, diketopiperazines, and sterols. Notably, several detected compounds, such as phenethyl alcohol, 2,4-di-tert-butylphenol, lauric acid, palmitic acid, and the diketopiperazine cyclo(L-Pro-L-Val) (Table 3), have been widely documented for antibacterial, membrane-disruptive, or quorum-sensing-inhibitory effects. The predominance of membrane-active fatty acids, coupled with synergistic sterols like ergosterol, suggests that bacterial membrane perturbation may contribute to the observed antibacterial effects. These metabolite signatures could explain the antibacterial effects observed in diffusion assays.

Table 2. Minimum inhibitory concentration (MIC) and minimum bactericidal concentration (MBC) of the A1RA crude extract against multidrug-resistant bacteria

Bacterial isolates	MIC (µg/mL)	MBC (µg/mL)	Interpretation
Staphylococcus aureus (MRSA)	>512	>512	No inhibitory or bactericidal activity
Escherichia coli (ESBL)	>512	>512	No inhibitory or bactericidal activity
Klebsiella pneumoniae (ESBL)	>512	>512	No inhibitory or bactericidal activity
Acinetobacter baumannii (ESBL)	>512	>512	No inhibitory or bactericidal activity

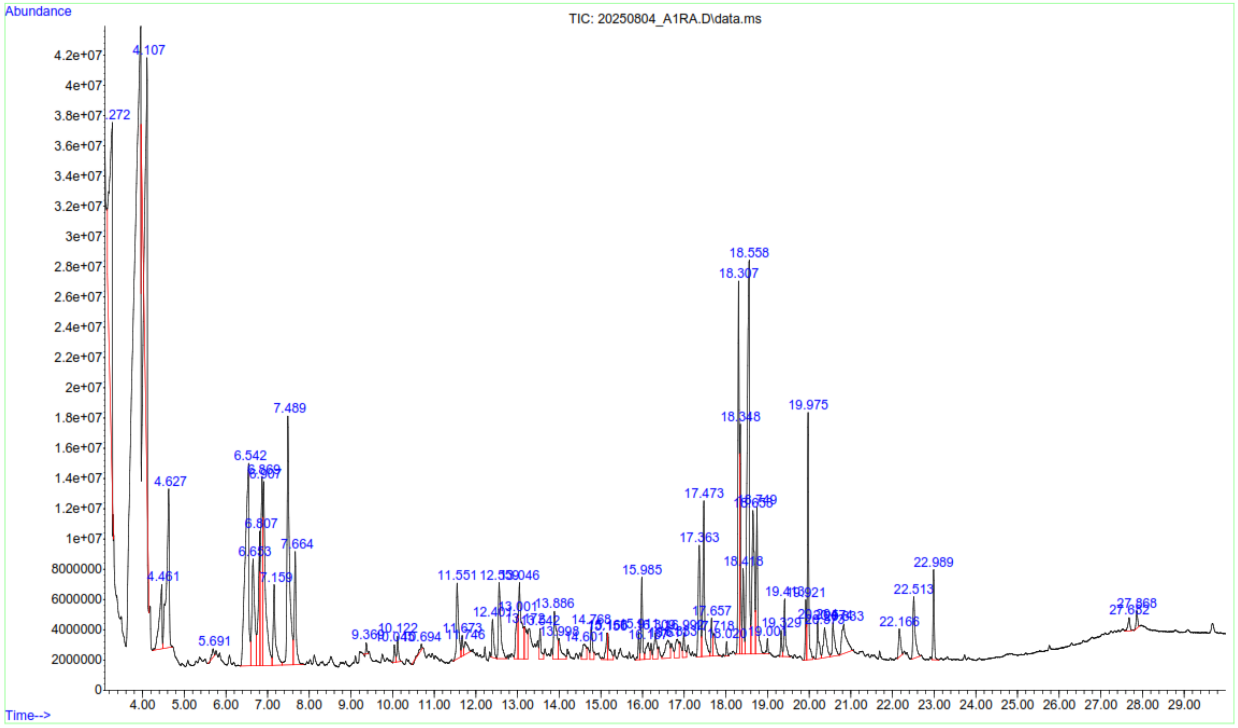

Figure 5. Total chromatograms detected in GC/MS ethyl acetate extract of A1RA

Table 3. Selected compounds identified by GC/MS analysis of A1RA crude extract and their reported antibacterial-related activities

Compounds	RT (min)	Molecular formula	Relative abundance	Reported activity	References
Phenethyl alcohol	7.51	$C_8H_{10}O$	5.48%	Increases bacterial membrane permeability	Kleinwächter et al. (2021)
Phenylacetic acid	11.65	$C_8H_8O_2$	1.45%	Acidifies cytoplasm, disrupts membrane	Cutro et al. (2019); Pan et al. (2022)
Cyclo(L-Pro-L-Val)	18.34	$C_{10}H_{16}N_2O$	2.31%	Quorum-sensing inhibition	Kapadia et al. (2022); Ren et al. (2022)
Cyclo(Phe-Pro)	29.50	$C_{14}H_{16}N_2O_2$	0.25%	Anti-quorum sensing, anti-biofilm	Li et al. (2022)
2,4-di-tert-butylphenol	18.59	$C_{14}H_{22}O$	7.87%	Membrane disruption, antioxidant	Halim et al. (2017); Kolyada et al. (2018)
Lauric acid (C12:0)	20.84	$C_{12}H_{24}O_2$	1.22%	Lytic to bacterial membranes	Zhao et al. (2022)
Myristic acid (C14:0)	23.61	$C_{14}H_{28}O_2$	1.03%	Protein synthesis inhibition, membrane damage	Beauchamp et al. (2024); Witwit et al. (2024)
Palmitic acid (C16:0)	22.48	$C_{16}H_{32}O_2$	1.26%	Alters membrane fluidity, anti-biofilm	Mozaheb et al. (2022); Santhakumari et al. (2017)
Oleic acid (C18:1)	25.15	$C_{18}H_{34}O_2$	0.24%	Inhibits FabI, essential for FA biosynthesis	Fage et al. (2020); Zhou et al. (2020)
Ergosterol	30.15	$C_{28}H_{44}O$	0.24%	Perturbs bacterial membranes, synergistic	Luchini et al. (2020)

Discussion

Antimicrobial resistance (AMR) is a growing global health challenge that motivates the exploration of under-investigated microbial resources, including mangrove-associated endophytic fungi, as potential sources of antibacterial metabolites. Mangrove ecosystems are characterized by high salinity, fluctuating environmental conditions, and nutrient limitation, which may promote the production of chemically diverse secondary metabolites not commonly observed in terrestrial isolates (Hastuti et al. 2020; Nizam et al. 2022). In this context, the isolation and characterization of mangrove-derived endophytic fungi remain timely and relevant to AMR research (Oliveira et al. 2024).

In the present study, four endophytic fungal isolates were obtained from surface-sterilized root tissues of *R. apiculata* collected from the Ngurah Rai Mangrove Forest, Bali, Indonesia. Based on preliminary screening using the agar-plug assay, isolate A1RA was selected for further identification and antibacterial evaluation due to its reproducible inhibition against at least one test bacterium. This selection approach is consistent with the exploratory nature of endophyte bioprospecting studies, where isolates are prioritized based on reproducible screening phenotypes.

Morphological characterization of isolate A1RA grown on Potato Dextrose Agar (PDA) at 28°C showed rapid colony expansion with a white, velvety to powdery surface and concentric zonation, while the reverse side displayed orange to reddish-orange pigmentation. Microscopic examination confirmed fungal hyphae and abundant conidia, and scanning electron microscopy further supported these observations. Overall, the colony appearance and microscopic traits were consistent with the genus *Talaromyces*. Similar observations were recorded by (Yilmaz et al. 2014; Chen et al. 2016; Jiang et al. 2018).

Molecular identification based on ITS rDNA sequencing confirmed isolate A1RA as *T. adpressus*, and phylogenetic analysis supported its placement within the *T. adpressus* clade. While *Talaromyces* species are widely recognized as prolific producers of secondary metabolites, information on *T. adpressus* from mangrove-associated environments remains limited. Previous studies have reported antibacterial activity from several *Talaromyces* isolates, including the production of polyketide-derived compounds and other bioactive secondary metabolites with inhibitory effects against bacterial pathogens (Zang et al. 2016; Vocadlova et al. 2023). Therefore, documenting *T. adpressus* as a mangrove root endophyte expands the ecological record of this species and contributes to current knowledge of fungal biodiversity in mangrove ecosystems.

The crude ethyl acetate extract of *T. adpressus* A1RA exhibited inhibitory activity against methicillin-resistant *S. aureus* (MRSA), ESBL-producing *E. coli*, *K. pneumoniae*, and *A. baumannii*. The extract produced inhibition zones of 13.22±1.13 mm against MRSA, 10.41 ±1.54 mm against ESBL-*E. coli*, 10.05±1.85 mm against ESBL-*A. baumannii*, and 9.98±0.11 mm against ESBL-*K. pneumoniae*. The observed activity against MRSA was particularly strong, consistent with evidence that Gram-positive bacteria are generally more susceptible to membrane-active fungal metabolites (Casillas-Vargas et al. 2021). Fatty acids, such as lauric and oleic acid, identified in the A1RA extract, are known to disrupt bacterial membranes and inhibit essential biosynthetic enzymes, mechanisms especially effective against Gram-positive pathogens (Sado-Kamdem et al. 2009; Park et al. 2018). MRSA represents a critical clinical challenge, and the ability of the extract to inhibit its growth further highlights the pharmacological relevance of these metabolites (Lan et al. 2024). However, the comparatively stronger inhibition observed in agar diffusion assays likely reflects localized high concentrations of lipophilic metabolites near the disc rather than sustained antibacterial activity in homogeneous liquid systems. Although inhibition zones against ESBL-producing *E. coli* and *K. pneumoniae* were smaller than those observed for MRSA, they remained statistically significant relative to controls, indicating meaningful antimicrobial activity. The reduced susceptibility of Gram-negative bacteria is expected due to the presence of an outer membrane that limits the penetration of hydrophobic molecules such as fatty acids and phenolic derivatives (Lundstedt et al. 2021; Hermansen et al. 2022). Importantly, measurable inhibition was also noted against ESBL-*A. baumannii*, a pathogen frequently associated with carbapenem resistance and nosocomial persistence. This observation suggests that localized exposure to sufficiently high concentrations of extract constituents may transiently disrupt bacterial growth, a phenomenon commonly reported for crude fungal and plant extracts even when MIC values remain high. Despite the relatively high MIC values obtained in this study, such differences between disc diffusion and broth microdilution are well recognized for crude natural extracts. Crude extracts comprise complex mixtures of compounds that may diffuse and accumulate locally in solid media, while requiring substantially higher, uniformly distributed concentrations to exert measurable effects in broth systems. Consistent with this, MIC and MBC values (>512 µg/mL) demonstrate that the crude extract does not exhibit strong bacteriostatic or bactericidal activity under standardized broth microdilution conditions, substantially limiting its direct therapeutic relevance in crude form.

GC-MS-based chemical profiling revealed a chemically diverse set of metabolites, providing mechanistic support for the antibacterial screening outcomes. Fatty acids, including lauric, myristic, palmitic, and oleic acids, are well-documented antimicrobial agents. Lauric acid has been reported to disrupt the cytoplasmic membrane of *S. aureus* (Qingyan et al. 2024), while oleic acid inhibits the enoyl-ACP reductase FabI, impairing membrane biosynthesis (Maltarollo et al. 2022). Palmitic and myristic acids alter membrane fluidity, inhibit electron transport, and reduce biofilm formation (Samartsev et al. 2011; Álvarez et al. 2015; Gomes et al. 2017; Santhakumari et al. 2017). Diketopiperazines (DKPs) such as cyclo(L-Pro-L-Val) and cyclo(Phe-Pro) detected in the extract are well-known fungal metabolites with quorum-sensing inhibitory properties. DKPs have been shown to disrupt acyl-homoserine lactone signalling systems and suppress bacterial virulence traits (Scoffone et al. 2016; Buroni et al. 2018; Mahan et al. 2020), and cyclo(Phe-Pro) has been reported to reduce virulence factor expression in *Pseudomonas aeruginosa* (Kumari and

Vijayan 2023). Phenolic compounds including phenylacetic acid, phenethyl alcohol, and 2,4-di-tert-butylphenol were also identified. Phenylacetic acid acidifies the cytoplasm and interferes with bacterial metabolic pathways (Russell et al. 2013), phenethyl alcohol disrupts membrane integrity and has long been used as an antimicrobial preservative (Kleinwächter et al. 2021), while 2,4-di-tert-butylphenol has been associated with both antioxidant and antibacterial activity in fungal extracts (Chawawisit et al. 2015; Yang et al. 2024). Ergosterol, although not strongly antibacterial alone, may act synergistically with fatty acids by enhancing membrane destabilization (Arellano et al. 2023; Park et al. 2022).

It is also possible that the modest antibacterial effects of individual fatty acids are amplified by interactions with sterols such as ergosterol, or with DKPs that modulate quorum sensing. Such synergistic interactions between membrane-active lipids and signalling inhibitors could contribute to the broad-spectrum inhibition observed in the disc-diffusion assay, even though MIC/MBC values remain high. However, the relatively weak MIC and MBC values indicate that these effects are unlikely to be driven by a single dominant compound and instead may arise from additive or synergistic interactions among multiple low-abundance metabolites. Although lauric, palmitic and oleic acids and ergosterol are widespread fungal constituents, their presence does not definitively identify them as the principal actives. The relatively weak MIC/MBC values suggest that other, less abundant metabolites or synergistic combinations may be responsible for the antibacterial effects.

Comparison with other *Talaromyces* species further contextualizes these results. *T. stipitatus*, *T. purpurogenus*, and *T. pinophilus* have been reported to produce terrein, azaphilones, and DKPs with antimicrobial activity (Zang et al. 2016; Vocadlova et al. 2023). Unlike *T. stipitatus* and *T. purpurogenus*, which are rich in azaphilones and terrein, our isolate from a mangrove environment produced a suite of saturated and unsaturated fatty acids. Such a fatty acid-dominated profile has not been reported from other *Talaromyces* endophytes, suggesting an adaptation to the saline, nutrient-poor mangrove habitat (Kasilingam et al. 2025). However, this compositional difference does not translate into strong antibacterial potency in crude extract form and should be interpreted primarily as an ecological rather than pharmacological distinction.

In conclusion, the antibacterial profile and metabolite composition of *T. adpressus* A1RA support its potential as a source of bioactive compounds relevant for AMR research. More importantly, the documentation of *T. adpressus* as a mangrove endophyte expands current knowledge of fungal biodiversity in mangrove ecosystems and provides a foundation for future targeted natural-product investigations rather than immediate antibacterial development. Although this study demonstrates meaningful antibacterial activity, several limitations exist. Future work should include bioassay-guided fractionation to isolate and test the activity of individual compounds, as well as combination studies to explore potential synergistic interactions. Nevertheless, the combined evidence from diffusion assays, metabolite composition, and ecological context supports the conclusion that A1RA possesses antibacterial constituents worthy of further purification and characterization.

ACKNOWLEDGEMENTS

This study was supported by the Fundamental Research Grant from the Ministry of Education, Culture, Research, and Technology of Indonesia for the 2025 fiscal year, awarded to Anak Agung Gede Indraningrat (Grant No. 129/C3/DT.05.00.PL/2025, 2166/LL8/AL.04/2025, and 702/Unwar/DPPM/PD-13/2025).

REFERENCES

Alhassan JAK, Abdallah CK. 2024. Health system interventions and responses to anti-microbial resistance: A scoping review of evidence from 15 african countries. PLoS Global Public Health 4 (9): e0003688. https://doi.org/10.1371/journal.pgph.0003688.

Álvarez R, López DJ, Casas J, Lladó V, Higuera M, Nagy T, Barceló M, Busquets X, Escribá PV. 2015. G protein-membrane interactions i: Gαi1 myristoyl and palmitoyl modifications in protein-lipid interactions and its implications in membrane microdomain localization. Biochim Biophys Acta Mol Cell Biol Lipids 1851 (11): 1511-1520. https://doi.org/10.1016/j.bbalip.2015.08.001.

Arellano H, Nardello-Rataj V, Szunerits S, Boukherroub R, Fameau AL. 2023. Saturated long chain fatty acids as possible natural alternative antibacterial agents: Opportunities and challenges. Adv Colloid Interface Sci 318: 102952. https://doi.org/10.1016/j.cis.2023.102952.

Bao M, Shi Y, Gong X, Guo Y, Wang J, Chen X, Liu L. 2025. New bioactive secondary metabolites from fungi: 2024. Mycology 16 (3): 961-987. https://doi.org/10.1080/21501203.2025.2526772.

Beauchamp E, Gamma JM, Cromwell CR, Moussa EW, Pain R, Kostiuk MA, Acevedo-Morantes C, Iyer A, Yap M, Vincent KM, Postovit LM. 2024. Multiomics analysis identifies oxidative phosphorylation as a cancer vulnerability arising from myristoylation inhibition. J Translational Med 22 (1): 431. https://doi.org/10.1186/s12967-024-05150-6.

Buenavista D, Purnobasuki H. 2023. People and mangroves: Biocultural utilization of mangrove forest ecosystem in southeast asia. J Mar Island Cult 12: 95-115. https://doi.org/10.21463/jmic.2023.12.2.07.

Buroni S, Scoffone VC, Fumagalli M, Makarov V, Cagnone M, Trespidi G, De Rossi E, Forneris F, Riccardi G, Chiarelli LR. 2018. Investigating the mechanism of action of diketopiperazines inhibitors of the *Burkholderia cenocepacia* quorum sensing synthase cepi: A site-directed mutagenesis study. Front Pharmacol 9: 836. https://doi.org/10.3389/fphar.2018.00836.

Cai R, Chen S, Long Y, Li C, Huang X, She Z. 2017. Depsidones from talaromyces stipitatus sk-4, an endophytic fungus of the mangrove plant *Acanthus ilicifolius*. Phytochem Lett 20: 196-199. https://doi.org/10.1016/j.phytol.2017.04.023.

Casillas-Vargas G, Ocasio-Malavé C, Medina S, Morales Guzmán C, Valle R, Carballeira N, Sanabria D. 2021. Antibacterial fatty acids: An update of possible mechanisms of action and implications in the development of the next-generation of antibacterial agents. Prog Lipid Res 82: 101093. https://doi.org/10.1016/j.plipres.2021.101093.

Chawawisit K, Bhoopong P, Phupong W, Lertcanawanichakul M. 2015. Anti-mrsa activity, mode of action and cytotoxicity of 2, 4-di-tert-butylphenol produced by *Streptomyces* sp. Kb1. Intl J Pharm Sci Rev Res 35 (1): 114-119.

Chen AJ, Sun BD, Houbraken J, Frisvad JC, Yilmaz N, Zhou YG, Samson RA. 2016. New Talaromyces species from indoor environments in China. Stud Mycol 84: 119-144. https://doi.org/10.1016/j.simyco.2016.11.003.

Chen, Tao H, Chen W, Yang B, Zhou X, Luo X, Liu Y. 2020. Recent advances in the chemistry and biology of azaphilones. RSC Adv 10 (17): 10197-10220. https://doi.org/10.1039/d0ra00894j.

Chen Y, Yang W, Zou G, Chen S, Pang J, She Z. 2019. Bioactive polyketides from the mangrove endophytic fungi *Phoma* sp. Sysu-sk-7. Fitoterapia 139: 104369. https://doi.org/10.1016/j.fitote.2019.104369.

Cutro AC, Disalvo EA, Frías MA. 2019. Effects of phenylalanine on the liquid-expanded and liquid-condensed states of phosphatidylcholine monolayers. Lipid Insights 12: 1-9. https://doi.org/10.1177/1178635318820923.

Dadgostar P. 2019. Antimicrobial resistance: Implications and costs. Infect Drug Resist 12: 3903-3910. https://doi.org/10.2147/idr.S234610.

Fage CD, Lathouwers T, Vanmeert M, Gao LJ, Vrancken K, Lammens EM, Weir AN, Degroote R, Cuppens H, Kosol S, Simpson TJ. 2020. The kalimantacin polyketide antibiotics inhibit fatty acid biosynthesis in *Staphylococcus aureus* by targeting the enoyl-acyl carrier protein binding site of fabi. Angewandte Chemie - Intl Ed 59 (26): 10549-10556. https://doi.org/10.1002/anie.201915407.

Galindo-Solís JM, Fernández FJ. 2022. Endophytic fungal terpenoids: Natural role and bioactivities. Microorganisms 10 (2): 339. https://doi.org/10.3390/microorganisms10020339.

Genilloud O. 2019. Natural products discovery and potential for new antibiotics. Curr Opin Microbiol 51: 81-87. https://doi.org/10.1016/j.mib.2019.10.012.

Gomes LC, Moreira JMR, Araújo JDP, Mergulhão FJ. 2017. Surface conditioning with *Escherichia coli* cell wall components can reduce biofilm formation by decreasing initial adhesion. AIMS Microbiol 3 (3): 613-628. https://doi.org/10.3934/microbiol.2017.3.613.

Guerrero JJ, General M, Balendres MA, Tan M, Buiza M, Huyop F. 2025. Medicines in medicines: Challenges and prospects in drug discovery from fungal endophytes of medicinal plants in Southeast Asia. J Trop Life Sci 15: 315-342. https://doi.org/10.11594/xvfdnn97.

Gulumbe BH, Haruna UA, Almazan JU, Ibrahim IH, Faggo AA, Bazata AY. 2022. Combating the menace of antimicrobial resistance in Africa: A review on stewardship, surveillance and diagnostic strategies. Biol Proced Online 24: 19. https://doi.org/10.1186/s12575-022-00182-y.

Halim NA, Razak SBA, Simbak N, Seng CT. 2017. 2,4-di-tert-butylphenol-induced leaf physiological and ultrastructural changes in chloroplasts of weedy plants. S Afr J Bot 112: 89-94. https://doi.org/10.1016/j.sajb.2017.05.022.

Hastuti E, Izzati M, Darmanti S. 2020. The impact of mangrove plantation in ponds on the secondary metabolite content. J Phys: Conf Ser 1524: 012055. https://doi.org/10.1088/1742-6596/1524/1/012055.

Hermansen S, Linke D, Leo JC. 2022. Transmembrane β-barrel proteins of bacteria: From structure to function. Adv Protein Chem Struct Biol 128: 113-161. https://doi.org/10.1016/bs.apcsb.2021.07.002.

Jiang XZ, Yu ZD, Ruan YM, Wang L. 2018. Three new species of *Talaromyces* sect. *Talaromyces* discovered from soil in China. Sci Rep 8 (1): 4932. https://doi.org/10.1038/s41598-018-23370-x.

Kadariswantiningsih IN, Rampengan DD, Ramadhan RN, Idrisova A, Idrisov B, Empitu MA. 2025. Antibiotic resistance in Indonesia: A systematic review and meta-analysis of extended-spectrum beta-lactamase-producing bacteria (2008-2024). Trop Med Intl Health 30 (4): 246-259. https://doi.org/10.1111/tmi.14090.

Kapadia C, Kachhdia R, Singh S, Gandhi K, Poczai P, Alfarraj S, Ansari MJ, Gafur A, Sayyed RZ. 2022. *Pseudomonas aeruginosa* inhibits quorum-sensing mechanisms of soft rot pathogen *Lelliottia amnigena* rce to regulate its virulence factors and biofilm formation. Front Microbiol 13: 977669. https://doi.org/10.3389/fmicb.2022.977669.

Kasilingam N, Muthusamy S, Duraisamy K. 2025. Production and biological characterization of nanoparticles from mangrove-associated microorganisms. Mangrove microbiome: Diversity and bioprospecting. Springer Nature Singapore, Singapore. https://doi.org/10.1007/978-981-96-2602-1_24.

Keller NP. 2019. Fungal secondary metabolism: Regulation, function and drug discovery. Nat Rev Microbiol 17 (3): 167-180. https://doi.org/10.1038/s41579-018-0121-1.

Kleinwächter IS, Pannwitt S, Centi A, Hellmann N, Thines E, Bereau T, Schneider D. 2021. The bacteriostatic activity of 2-phenylethanol derivatives correlates with membrane binding affinity. Membranes 11 (4): 254. https://doi.org/10.3390/membranes11040254.

Kolyada MN, Osipova VP, Berberova NT, Shpakovsky DB, Milaeva ER. 2018. Antioxidant activity of 2,6-di-tert-butylphenol derivatives in lipid peroxidation and hydrogen peroxide decomposition by human erythrocytes in vitro. Russ J Gen Chem 88 (12): 2513-2517. https://doi.org/10.1134/S1070363218120095.

Kumari PS, Vijayan V. 2023. Synergistic activity of cyclo(phe-pro) antibiotic from streptomyces violascens vs in reducing the drug resistance burden of clinically significant pathogens. J Biol Act Prod Nat 12 (6): 450-460. https://doi.org/10.1080/22311866.2022.2162579.

Lan T, Zhang B, Liu JL, Jia Q, Gao J, Cao L, Yan J, Li BL, Xie XJ, Xu YH, Wen HM. 2024. Prevalence and antibiotic resistance patterns of methicillin-resistant *Staphylococcus aureus* (MRSA) in a hospital setting: A retrospective study from 2018 to 2022. Indian J Microbiol 64 (3): 1035-1043. https://doi.org/10.1007/s12088-024-01228-3.

Li J, Zhang Q, Zhao J, Zhang H, Chen W. 2022. *Streptococcus mutans* and *Candida albicans* biofilm inhibitors produced by *Lactiplantibacillus plantarum* ccfm8724. Curr Microbiol 79 (5): 143. https://doi.org/10.1007/s00284-022-02833-5.

Liana P, Binti Chahril N, Nita S, Umar TP. 2022. Prevalence of extended-spectrum beta lactamase-producing microorganisms in Dr. Mohammad Hoesin hospital Palembang. Indones J Clin Pathol Med Lab 28 (3): 263-268. https://doi.org/10.24293/ijcpml.v28i3.1897.

Liao C, Doilom M, Jeewon R, Hyde KD, Manawasinghe IS, Chethana KT, Balasuriya A, Thakshila SA, Luo M, Mapook A, Htet ZH. 2025. Challenges and update on fungal endophytes: Classification, definition, diversity, ecology, evolution and functions. Fungal Diver 131 (1): 301-367. https://doi.org/10.1007/s13225-025-00550-5.

Luchini A, Delhom R, Cristiglio V, Knecht W, Wacklin-Knecht H, Fragneto G. 2020. Effect of ergosterol on the interlamellar spacing of deuterated yeast phospholipid multilayers. Chem Phys Lipids 227: 104873. https://doi.org/10.1016/j.chemphyslip.2020.104873.

Lundstedt E, Kahne D, Ruiz N. 2021. Assembly and maintenance of lipids at the bacterial outer membrane. Chem Rev 121 (9): 5098-5123. https://doi.org/10.1021/acs.chemrev.0c00587.

Madhavan C, Meera SP, Kumar A. 2025. Anatomical adaptations of mangroves to the intertidal environment and their dynamic responses to various stresses. Biol Rev 100 (3): 1019-1046. https://doi.org/10.1111/brv.13172.

Mahan K, Martinmaki R, Larus I, Sikdar R, Dunitz J, Elias M. 2020. Effects of signal disruption depends on the substrate preference of the lactonase. Front Microbiol 10: 3003. https://doi.org/10.3389/fmicb.2019.03003.

Maltarollo VG, Shevchenko E, Lima IDDM, Cino EA, Ferreira GM, Poso A, Kronenberger T. 2022. Do go chasing waterfalls: Enoyl reductase (fabi) in complex with inhibitors stabilizes the tetrameric structure and opens water channels. J Chem Inf Model 62 (22): 5746-5761. https://doi.org/10.1021/acs.jcim.2c01178.

Mozaheb N, Van Der Smissen P, Opsomer T, Mignolet E, Terrasi R, Paquot A, Larondelle Y, Dehaen W, Muccioli GG, Mingeot-Leclercq MP. 2022. Contribution of membrane vesicle to reprogramming of bacterial membrane fluidity in *Pseudomonas aeruginosa*. mSphere 7 (3): e00187-22. https://doi.org/10.1128/msphere.00187-22.

Nagarajan K, Ibrahim B, Bawadikji AA, Lim JW, Tong WY, Leong CR, Khaw KY, Tan WN. 2021. Recent developments in metabolomics studies of endophytic fungi. J Fungi 8 (1): 28. https://doi.org/10.3390/jof8010028.

Nasution SSA, Elfita, Widjajanti H, Ferlinahayati. 2024. Diversity, bioactivity, and phytochemistry of endophytic fungi in various organs of nipa palm (*Nypa fruticans*) mangrove. Biodiversitas 25: 3928-3942. https://doi.org/10.13057/biodiv/d251053.

Newman DJ, Cragg GM. 2020. Natural products as sources of new drugs over the nearly four decades from 01/1981 to 09/2019. J Nat Prod 83 (3): 770-803. https://doi.org/10.1021/acs.jnatprod.9b01285.

Nicoletti R, Bellavita R, Falanga A. 2023. The outstanding chemodiversity of marine-derived Talaromyces. Biomolecules 13 (7): 1021. https://doi.org/10.3390/biom13071021.

Nizam A, Meera SP, Kumar A. 2022. Genetic and molecular mechanisms underlying mangrove adaptations to intertidal environments. iScience 25 (1): 103547. https://doi.org/10.1016/j.isci.2021.103547.

Oliveira M, Antunes W, Mota S, Madureira-Carvalho Á, Dinis-Oliveira RJ, Dias da Silva D. 2024. An overview of the recent advances in antimicrobial resistance. Microorganisms 12 (9): 1920. https://doi.org/10.3390/microorganisms12091920.

Ortega HE, Torres-Mendoza D, Cubilla-Rios L. 2025. Antibacterial compounds isolated from endophytic fungi reported from 2021 to 2024. Antibiotics 14 (7): 644. https://doi.org/10.3390/antibiotics14070644.

Pan H, Xiao Y, Xie A, Li Z, Ding H, Yuan X, Sun R, Peng Q. 2022. The antibacterial mechanism of phenylacetic acid isolated from *Bacillus megaterium* l2 against *Agrobacterium tumefaciens*. PeerJ 10: e14304. https://doi.org/10.7717/peerj.14304.

Park KM, Lee SJ, Yu H, Park JY, Jung HS, Kim K, Lee CJ, Chang PS. 2018. Hydrophilic and lipophilic characteristics of non-fatty acid moieties: Significant factors affecting antibacterial activity of lauric

acid esters. Food Sci Biotechnol 27 (2): 401-409. https://doi.org/10.1007/s10068-018-0353-x.

Park S, Lee JH, Kim YG, Hu L, Lee J. 2022. Fatty acids as aminoglycoside antibiotic adjuvants against *Staphylococcus aureus*. Front Microbiol 13: 876932. https://doi.org/10.3389/fmicb.2022.876932.

Qingyan L, Susu S, Shuanglin L, Youhua X, Haiyang Y, Yuan Y. 2024. Antibacterial activity and mechanism of lauric acid against *Staphylococcus aureus* and its application in infectious cooked chicken. Foodborne Pathog Dis 21 (12): 766-773. https://doi.org/10.1089/fpd.2024.0063.

Ren Z, Xie L, Okyere SK, Wen J, Ran Y, Nong X, Hu Y. 2022. Antibacterial activity of two metabolites isolated from endophytic bacteria *Bacillus velezensis* ea73 in *Ageratina adenophora*. Front Microbiol 13: 860009. https://doi.org/10.3389/fmicb.2022.860009.

Russell WR, Duncan SH, Scobbie L, Duncan G, Cantlay L, Calder AG, Anderson SE, Flint HJ. 2013. Major phenylpropanoid-derived metabolites in the human gut can arise from microbial fermentation of protein. Mol Nut Food Res 57 (3): 523-535. https://doi.org/10.1002/mnfr.201200594.

Sado-Kamdem SL, Vannini L, Guerzoni ME. 2009. Effect of α-linolenic, capric and lauric acid on the fatty acid biosynthesis in *Staphylococcus aureus*. Intl J Food Microbiol 129 (3): 288-294. https://doi.org/10.1016/j.ijfoodmicro.2008.12.010.

Samartsev VN, Marchik EI, Shamagulova LV. 2011. Free fatty acids as inducers and regulators of uncoupling of oxidative phosphorylation in liver mitochondria with participation of adp/atp- and aspartate/glutamate-antiporter. Biochemistry (Moscow) 76 (2): 217-224. https://doi.org/10.1134/S0006297911020088.

Santajit S, Indrawattana N. 2016. Mechanisms of antimicrobial resistance in eskape pathogens. BioMed Res Intl 2016 (1): 2475067. Https://doi.org/10.1155/2016/2475067.

Santhakumari S, Nilofernisha NM, Ponraj JG, Pandian SK, Ravi AV. 2017. In vitro and in vivo exploration of palmitic acid from *Synechococcus elongatus* as an antibiofilm agent on the survival of *Artemia franciscana* against virulent vibrios. J Invert Pathol 150: 21-31. https://doi.org/10.1016/j.jip.2017.09.001.

Scoffone VC, Chiarelli LR, Makarov V, Brackman G, Israyilova A, Azzalin A, Forneris F, Riabova O, Savina S, Coenye T, Riccardi G. 2016. Discovery of new diketopiperazines inhibiting *Burkholderia cenocepacia* quorum sensing in vitro and in vivo. Sci Rep 6 (1): 32487. https://doi.org/10.1038/srep32487.

Shi Y, Ji M, Dong J, Shi D, Wang Y, Liu L, Feng S, Liu L. 2024. New bioactive secondary metabolites from fungi: 2023. Mycology 15 (3): 283-321. https://doi.org/10.1080/21501203.2024.2354302.

Tacconelli E, Carrara E, Savoldi A, Harbarth S, Mendelson M, Monnet DL, Pulcini C, Kahlmeter G, Kluytmans J, Carmeli Y, Ouellette M. 2018. Discovery, research, and development of new antibiotics: The who priority list of antibiotic-resistant bacteria and tuberculosis. Lancet Infect Dis 18 (3): 318-327. https://doi.org/10.1016/s1473-3099(17)30753-3.

Vocadlova K, Lüddecke T, Patras MA, Marner M, Hartwig C, Benes K, Matha V, Mraz P, Schäberle TF, Vilcinskas A. 2023. Extracts of *Talaromyces purpureogenus* strains from *Apis mellifera* bee bread inhibit the growth of paenibacillus spp. In vitro. Microorganisms 11 (8): 2067. https://doi.org/10.3390/microorganisms11082067.

Witwit H, Betancourt CA, Cubitt B, Khafaji R, Kowalski H, Jackson N, Ye C, Martinez-Sobrido L, de la Torre JC. 2024. Cellular n-myristoyl transferases are required for mammarenavirus multiplication. Viruses 16 (9): 1362. https://doi.org/10.3390/v16091362.

Yang L, Wang R, Lin W, Li B, Jin T, Weng Q, Zhang M, Liu P. 2024. Efficacy of 2,4-di-tert-butylphenol in reducing *Ralstonia solanacearum* virulence: Insights into the underlying mechanisms. ACS Omega 9 (4): 4647-4655. https://doi.org/10.1021/acsomega.3c07887.

Yilmaz N, Visagie CM, Houbraken J, Frisvad JC, Samson RA. 2014. Polyphasic taxonomy of the genus *Talaromyces*. Stud Mycol 78: 175-341. https://doi.org/10.1016/j.simyco.2014.08.001.

Zang Y, Genta-Jouve G, Retailleau P, Escargueil A, Mann S, Nay B, Prado S. 2016. Talaroketals a and b, unusual bis(oxaphenalenone) spiro and fused ketals from the soil fungus *Talaromyces stipitatus* atcc 10500. Org Biomol Chem 14 (9): 2691-2697. https://doi.org/10.1039/c5ob02657a.

Zhai M-M, Li J, Jiang C-X, Shi Y-P, Di D-L, Crews P, Wu Q-X. 2016. The bioactive secondary metabolites from Talaromyces species. Nat Prod Bioprospect 6 (1): 1-24. https://doi.org/10.1007/s13659-015-0081-3.

Zhang J, Zhu Y, Si J, Wu L. 2022. Metabolites of medicine food homology-derived endophytic fungi and their activities. Curr Res Food Sci 5: 1882-1896. https://doi.org/10.1016/j.crfs.2022.10.006.

Zhao D, Wang S, Hu Y, Liu X, Tao J, Sagratini G, Xiang Q. 2022. Insight into the antibacterial activity of lauric arginate against *Escherichia coli* O157:H7: Membrane disruption and oxidative stress. LWT 162: 113449. https://doi.org/10.1016/j.lwt.2022.113449.

Zheng M, Xiao Y, Li Q, Lai Y, Dai B, Zhang M, Kang X, Tong Q, Wang J, Chen C, Zhu H. 2023. Cytotoxic ergosteroids from a strain of the fungus *Talaromyces adpressus*. J Nat Prod 86 (9): 2081-2090. https://doi.org/10.1021/acs.jnatprod.3c00089.

Zhou J, Zhang L, Zhang L. 2020. Advances on mechanism and drug discovery of type-ii fatty acid biosynthesis pathway. Acta Chim Sin 78 (12): 1383-1398. https://doi.org/10.6023/A20070299.